Riser-Soil Interaction: Local Dynamics at TDP and a Discussion on the Eigenvalue and the VIV Problems

Celso P. Pesce
e-mail: ceppesce@usp.br
Fluid-Structure Interaction and Offshore
Mechanics Laboratory,
Department of Mechanical Engineering,
Escola Politécnica,
University of São Paulo,
São Paulo 05508-900, Brazil

Clóvis de A. Martins
Fluid-Structure Interaction and Offshore
Mechanics Laboratory,
Department of Mechanical Engineering,
Escola Politécnica,
University of São Paulo,
São Paulo 05508-900, Brazil
and
NDF—Nucleus for Dynamics and Fluids,
Av. Prof. Mello Moraes 2231,
São Paulo, SP 05508-900, Brazil

Lauro M. Y. da Silveira
NDF—Nucleus for Dynamics and Fluids,
Av. Prof. Mello Moraes 2231,
São Paulo, SP 05508-900, Brazil

The eigenvalue problem of risers is of utmost importance, particularly if vortex-induced vibration (VIV) is concerned. Design procedures rely on the determination of eigenvalues and eigenmodes. Natural frequencies are not too sensitive to the proper consideration of boundary condition, within a certain extent where dynamics at the touchdown area (TDA) may be modeled as dominated by the dynamics of the suspended part. However, eigenmodes may be strongly affected in this region because, strictly speaking, this is a nonlinear one-side (contact-type) boundary condition. Actually, we shall consider a nonlinear eigenvalue problem. Locally, at TDA, riser flexural rigidity and soil interaction play important roles and may affect the dynamic curvature. Extending and merging former analytical solutions on touchdown point (TDP) dynamics and on the eigenvalue problem, obtained through asymptotic and perturbation methods, the present work critically address soil and bending stiffness effects a little further. As far as linear soil stiffness and planar dynamics hypotheses may be considered valid, it is shown that penetration in the soil is small and that its effect does not change significantly the bending loading that is mainly caused by the cyclic excursion of the TDP and corresponding dynamic tension. A comparison of the analytical results with a full nonlinear time-domain simulation shows a remarkable agreement for a typical steel catenary riser. The WKB approximation for the eigenvalue problem gives good estimates for TDP excursion. As the dynamic tension caused solely by VIV is very small, the merged analytical solution may be used as a first estimate of the curvature variation at TDP in the cases of current perpendicular to the "riser plane." [DOI: 10.1115/1.2151205]

Keywords: riser dynamics, eigenvalue, eigenmodes, WKB, asymptotic methods, soil interaction, TDP, VIV

Introduction

Dynamics of risers still demands research efforts. An extensive, though not so recent, review on modeling and analysis methods can be found in Patel and Seyed [1] who pointed out a number of research topics that should deserve special consideration. One of them is related to the riser-soil contact modeling. This topic "awaits a comprehensive and consistent treatment, where nonlinear effects would be properly taken into account. Embedding, trenching or shocking should be cited as some of important phenomena not yet properly incorporated in most design procedures, deserving much more investigations," Pesce and Martins [2].

Recently, a major research effort has been completed in soil-riser interaction modeling, particularly with emphasis on such highly nonlinear effects, combining experimental, analytical, and numerical methods (see, e.g., [3–5]). CARISIMA [3,4] is a comprehensive empirical model based on extensive experimental work, considering vertical suction, lateral resistance, pipe penetration, and trenching. Particularly, those authors point out that the "application of the model has a strong effect on the computed fatigue lifetimes." Actually, this effect is more related to trenching, suction, and embedding than to the vertical (elastic) response of the soil.

Despite those highly complex nonlinear mechanisms, numerical riser-soil interaction modeling is usually restricted to springs (linear or not), sometimes taking into account the strongly nonlinear one-side (contact-type) boundary condition. In this context, the usual "beam on a linearly elastic foundation" approximation would be certainly questionable. However, as far as linear soil stiffness and planar dynamics hypotheses may be considered valid, the present analysis will show that the soil penetration effect does not significantly change the bending loading caused by the cyclic excursion of the touchdown point (TDP). Embedding and other effects apart, the TDP excursion may be said to be the most important factor in the fatigue damage of steel catenary risers (SCR). In this sense, the quasi-static analytical solution provided in the present paper will prove to be quite valuable and not only as a benchmark for numerical schemes. Questionable as it may be, the linear elastic foundation approximation might be said to be valid at least for relatively stiff soils. As pointed out by Fontaine et al. [5] "for cycling loading, high values for the averaged vertical stiffness have been observed, despite the soil cohesion being low."

Common design practices make extensive use of numerical methods to account for the soil effect on riser dynamics, at TDA. On the other hand, asymptotic and perturbation methods have been used to deal with the riser-soil interaction problem. Based on previous works by Triantafyllou et al. [6] and Irvine [7], Aranha et al. [8] derived an analytical solution to represent the nonlinear dynamic behavior of a riser at TDA. Although experimentally confirmed in Pesce et al. [9], this work was restricted to the (important) rigid-soil case. The soil rigidity effect on the *static* con-

figuration of a catenary riser was addressed analytically in Pesce et al. [10]. Although it was relatively straightforward, the extension of that analysis to the dynamic case has not yet been presented.

Another very important subject in riser dynamics is the eigenvalue problem. The eigenvalue problem turns out to be of utmost importance when design tasks concern vortex-induced vibrations (VIV). Because direct nonlinear numerical simulations are extremely time-consuming, modern design practices make extensive use of frequency-domain methods.

Design procedures rely on the determination of eigenvalues and eigenmodes. Strictly, we should consider a nonlinear eigenvalue problem, taking into account the whole pipe, from the anchor to the floating unit and, properly, the contact problem. Or else, an effective participation length on the soil might be considered.

If, instead, only the suspended part is analyzed, the soil interaction must be accounted for separately. As the actual TDP displacement is small compared to the suspended length $L(t)$, eigenfrequencies are not expected to be too sensitive on boundary condition at the TDA, if the soil rigidity is considered large enough.

Furthermore, in VIV analysis, lock-on usually occurs for high values of eingenfrequencies. In typical deep-water SCR cases, eigenmodes higher than the 20th are likely to be excited. In these situations, the global dynamics, due to motions imposed by the floating unit, is relatively slow, such that eigenvalues could be considered modulated in time, due to the variation in span and tension. This could be formalized through the classical method of multiple scales (see, e.g., [11]).

Moreover, as for the suspended part the riser bending stiffness effect is only dominant inside a small boundary layer at TDA, an asymptotic solution for the eigenvalue problem of a curved and tensioned string can be applied (see, e.g., [12]). This solution was first derived by Triantafyllou [13] for taut inclined cables and, in the specific area of riser dynamics, by Pesce et al. [14]. In this latter work the riser was considered nonextensible. A simple analytical (WKB) closed-form solution was obtained, given the function describing the static effective tension along the riser length. Such an analytical solution does not take into account either the bending stiffness of the riser or the soil rigidity, which locally affects the dynamic curvature, at TDA. These effects must be incorporated.

Two paths could then be followed. The first one would consist of linearizing the eigenvalue problem around the static configuration, matching the solution on the soil with the asymptotic solution, valid on the suspended part, through a standard boundary layer technique.

A second path is chosen, however. The static boundary layer solution in elastic soil, presented in Pesce et al. [10] is extended to construct a quasi-static nonlinear solution, similar to that presented in Aranha et al. [8] for the rigid-soil case. This local quasi-static solution is driven by relatively slow[1] functions that describe dynamic tension and TDP excursion, which can be easily evaluated from the asymptotic approximation.

Local Subcritical Dynamics of a Catenary Riser Laid on Linear Elastic Soil

For simplicity, consider the planar problem of a free-hanging catenary riser laid on a linear elastic soil (Fig. 1). Let k be the soil rigidity per unit length and penetration. Let also $y(s,t)$ be the local solution for the *elastica* such that $y_r = -q/k$; $s/\lambda \to -\infty$ is the static offset (penetration in the soil) far away from the TDP. The immersed weight per unit length is q, $\lambda = \sqrt{EI/T_0}$ is the flexural boundary layer length scale, and T_0 is the static tension at TDP. A local analytical solution was derived by Pesce et al. [10] for the static problem. There, the solution on the soil is matched to the
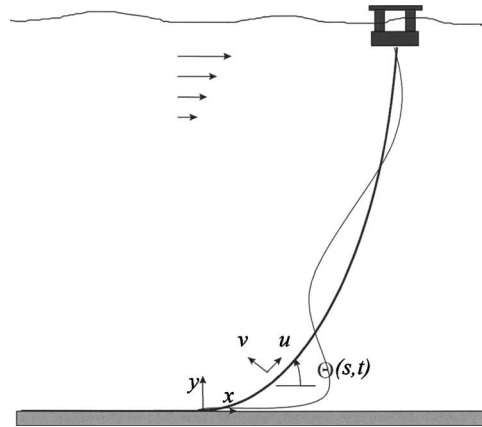

Fig. 1 Two-dimensional catenary riser problem. Displacements exaggerated

boundary layer solution valid for the suspended part, enforcing continuity on shear. This result can be extended to a subcritical dynamic regime, i.e., under the hypothesis of no impact against the soil.

Quasi-Static Equation on the Soil. As said before, we restrict ourselves to the planar problem. Consider the dynamic solution for the corresponding problem of a heavy cable to be known. Let $\chi_0 = q/T_0$ be the static curvature of the cable at TDP. Note that *all static information is contained in the static tension T_0 and all dynamic information in the dynamic tension, $\tau_0(t)$ and in the excursion of the cable TDP, $x_0(t)$*. Now, let the coordinate $s_K(t)$ define the actual TDP position, here taken as the point where the *elastica* touches the bottom, i.e., $y(s_K) = 0$. For simplicity we consider a nondetachment condition from the soil, for $s \leqslant s_K$. If the soil is not too soft, we can locally take, $\theta \cong dy/dx$ and with a second-order error in θ, $s \cong x$ and $\chi(s) \cong \chi(x) \cong d^2y/dx^2$.

Consider now the local nondimensional coordinates $\xi = x/\lambda$, $\eta(\xi,t) = y(s,t)/\lambda$ and the (rapidly varying) nondimensional local time scale $\hat{t} = tc_0/\lambda$, being $c_0 = \sqrt{T_0/(m+m_a)}$ the local cable transversal wave celerity, where m and m_a, are mass and added mass per unit length. Note that $\xi_K(\hat{t}) = s_K(\hat{t})/\lambda$ defines the actual instantaneous TDP position. Let, also, K be the nondimensional soil rigidity parameter,

$$K = \frac{kEI}{T_0^2} = \frac{k\lambda^2}{T_0} = \frac{k\lambda^4}{EI} = \chi_0\lambda\frac{k\lambda}{q} \tag{1}$$

With no loss of generality, we may disregard the nondimensional static penetration in the soil, far away from the TDP, given by $\eta_r = y_r/\lambda = -q/k\lambda = -\chi_0\lambda/K$. Therefore, the dynamic equilibrium equation for a bar, acted by dynamic tension and laid on a linear elastic soil, can be written in nondimensional form as

$$\frac{\partial^4\eta}{\partial\xi^4} - f(\hat{t})\frac{\partial^2\eta}{\partial\xi^2} + K\eta = -\frac{\partial^2\eta}{\partial\hat{t}^2} \tag{2}$$

where, $f(\hat{t}) = 1 + \tau_0(\hat{t})/T_0$, $\tau_0(\hat{t}) = \tau(0,\hat{t})$ is the local nondimensional dynamic tension function, which will be considered to be positive, precluding compression.[2]

Let us now consider that the dynamics of the suspended part governs the local dynamics. In other words, a global (slow) time scale, related to the geometric rigidity of the suspended part, can be defined as $t = tc_0/L = \varepsilon\hat{t}$, being $\varepsilon = \lambda/L$ a small quantity and L the cable suspended length in the static configuration. Equation (2) may be written

---

[1]If compared to the dynamics of the supported part.

[2]For dynamic compression, see [15,16].

$$\frac{\partial^4 \eta}{\partial \xi^4} - f(t)\frac{\partial^2 \eta}{\partial \xi^2} + K\eta = -\varepsilon^2 \frac{\partial^2 \eta}{\partial t^2} \qquad (3)$$

Therefore, with an error of order ε^2, a quasi-static approximate equation, in the slow time scale t, reads[3]

$$\eta^{IV} - f(t)\eta^{II} + K\eta = 0 \qquad (4)$$

Taking $f(t) > 0$, Eq. (4) has a standard homogeneous solution,

$$\eta(\xi,t) = \sum_{j=1}^{4} A_j e^{\varpi_j(t)[\xi - \xi_K(t)]}; \quad \xi \leqslant \xi_K(t) \qquad (5)$$

with complex eigenvalues

$$\varpi_j(t) = \pm\left(\frac{\sqrt{f(t)} \pm [f(t) - 4K]^{1/2}}{2}\right)^{1/2} \qquad (6)$$

However, under relatively small variations of tension, we have $f(t) \approx O(1)$. Additionally, we take a sufficiently rigid soil, such that $K \gg 1$. This, in fact, corresponds to typical situations for steel catenary risers leading, for the boundary conditions $\eta[\xi_K(t)] = 0$; $\lim_{\xi \to -\infty} \eta(\xi) = 0$, to a simple approximate quasi-static solution

$$\eta(\xi,t) = C(t)\exp\left(\frac{K^{1/4}}{\sqrt{2}}[\xi - \xi_K(t)]\right)\sin\left(\frac{K^{1/4}}{\sqrt{2}}[\xi - \xi_K(t)]\right)$$

$$\text{valid for } [\xi - \xi_K(t)] \leqslant 0 \qquad (7)$$

Note that there are two unknowns, $C(t)$ and $\xi_K(t)$, that must be determined by matching the soil solution with the suspended part (local) solution.

Subcritical Dynamic Solution in the Suspended Part. It was shown by Triantafyllou et al. [6] that a shock condition for a cable against the soil holds whenever the local Mach number, $M = \dot{x}_0/c_0$ is > 1. This assertion can be physically interpreted as the lack of time for the cable to properly adjust its geometric form. Conversely, the condition $M < 1$ is said to be a *subcritical dynamic regime*. For this latter situation, it has also been shown by Aranha et al.,[8] that *the inertia terms can be locally disregarded*, with an error of the order of $M^2 \ll 1$.

For convenience, we take $\xi = 0$ as the static TDP position of the corresponding cable case. Therefore, $\xi_0(t) = x_0(t)/\lambda$. Let $X(\xi) = \chi(\xi)\lambda$ be the nondimensional curvature. $X_0 = \chi_0\lambda$ is the cable static curvature at TDP, usually a small quantity, of order 5×10^{-3} for a SCR.

Merging the reasoning presented in Aranha et al. [8] and Pesce et al. [10], the local (boundary layer) quasi-static nondimensional solution for the curvature, valid in the suspended part, $(\xi - \xi_K(t)) \geqslant 0$, may be written

$$\eta^{II}(\xi,t) = \frac{X_0}{f(t)}\{1 - A_1(t)\exp[-b(t)(\xi - \xi_K(t))]\} \qquad (8)$$

such that angle and *elastica* nondimensional functions are given, respectively, by

$$\eta^{I}(\xi,t) = \frac{X_0}{f(t)}\left([\xi - \xi_0(t)] + \frac{A_1(t)}{\sqrt{f(t)}}\exp\{-\sqrt{f(t)}[\xi - \xi_K(t)]\}\right) \qquad (9)$$

$$\eta(\xi,t) = \frac{X_0}{f(t)}\left\{\frac{\xi^2 - \xi_K^2(t)}{2} - \xi_0(t)[\xi - \xi_K(t)]\right\}$$
$$+ \frac{X_0}{f(t)}\left(-\frac{A_1(t)}{f(t)}\exp\{-\sqrt{f(t)}[\xi - \xi_K(t)]\} + A_2(t)\right) \qquad (10)$$

and the nondimensional shear force by

---

[3] η^I indicates derivative with respect to the local coordinate ξ.

$$\eta^{III}(\xi,t) = \frac{X_0}{\sqrt{f(t)}}A_1(t)\exp\{-\sqrt{f(t)}[\xi - \xi_K(t)]\} \qquad (11)$$

Note that there are two additional unknown nondimensional functions, namely, $A_1(t)$ and $A_2(t)$. However, enforcing $\eta[\xi_K(t),t] \equiv 0$, we obtain from (10)

$$A_2(t) = \frac{A_1(t)}{f(t)} \qquad (12)$$

Matching Solutions. The solutions given in Eqs. (7) and (10) can be matched by equating derivatives up to third-order at $\xi = \xi_K(t)$. The following set of linear algebraic equations is then obtained:

$$\frac{K^{1/4}}{\sqrt{2}}C(t) = \frac{X_0}{f(t)}\left(\xi_K(t) - \xi_o(t) + \frac{A_1(t)}{\sqrt{f(t)}}\right)$$

$$K^{1/2}C(t) = \frac{X_0}{f(t)}[1 - A_1(t)]$$

$$\frac{K^{3/4}}{\sqrt{2}}C(t) = X_0\frac{A_1(t)}{\sqrt{f(t)}} \qquad (13)$$

Solving Eqs. (12) and (13) the unknowns $[C(t), A_1(t), A_2(t), \xi_K(t)]$ are readily determined as

$$C(t) = \frac{X_0}{\sqrt{f(t)}}\frac{\sqrt{2}}{K^{1/2}}\frac{1}{K^{1/4} + \sqrt{2f(t)}}$$

$$A_1(t) = \frac{K^{1/4}}{K^{1/4} + \sqrt{2f(t)}}$$

$$A_2(t) = \frac{1}{f(t)}\frac{K^{1/4}}{K^{1/4} + \sqrt{2f(t)}} \qquad (14)$$

and

$$\xi_K(t) = \xi_0(t) - \frac{K^{1/4}}{K^{1/4} + \sqrt{2f(t)}}\left(\frac{1}{\sqrt{f(t)}} - \frac{\sqrt{f(t)}}{K^{1/2}}\right) \qquad (15)$$

Therefore, closing the present local quasi-static analytical solution at TDA, we have

$$\eta(\xi,t) = \frac{X_0}{\sqrt{f(t)}}\frac{\sqrt{2}}{K^{1/2}}\frac{1}{K^{1/4} + \sqrt{2f(t)}}\exp\left(\frac{K^{1/4}}{\sqrt{2}}[\xi - \xi_K(t)]\right)$$

$$\times \sin\left(\frac{K^{1/4}}{\sqrt{2}}[\xi - \xi_K(t)]\right)$$

$$\text{valid for } [\xi - \xi_K(t)] \leqslant 0$$

and

$$\eta(\xi,t) = \frac{X_0}{f(t)}\left\{\frac{\xi^2 - \xi_K^2(t)}{2} - \xi_0(t)[\xi - \xi_K(t)]\right\}$$

$$+ \frac{X_0}{f(t)}\left[\frac{1}{f(t)}\frac{K^{1/4}}{K^{1/4} + \sqrt{2f(t)}}(1 - \exp\{-\sqrt{f(t)}[\xi - \xi_K(t)]\})\right]$$

$$\text{valid for } [\xi - \xi_K(t)] \geqslant 0 \qquad (16)$$

By taking $\xi_0(t) \equiv 0$ and $f(t) \equiv 1$, it can be easily shown that this solution recovers the static case, presented in Pesce et al. [10]. On the other hand, in the rigid-soil limit case, where $K \to \infty$, the present solution recovers the dynamic solution derived in Aranha et al. [8] and experimentally confirmed and presented in revised form in Pesce et al. [9].

For simplicity, TDP excursion is taken as $\xi_0(t) = x_0(t)/\lambda = a_0 \cos \omega t$ and the dynamic tension, in anti-phase, as $f(t) = 1 - \tau_0(t)/T_0 = 1 - \beta_0 \cos \omega t$. Soil is considered relatively soft, with
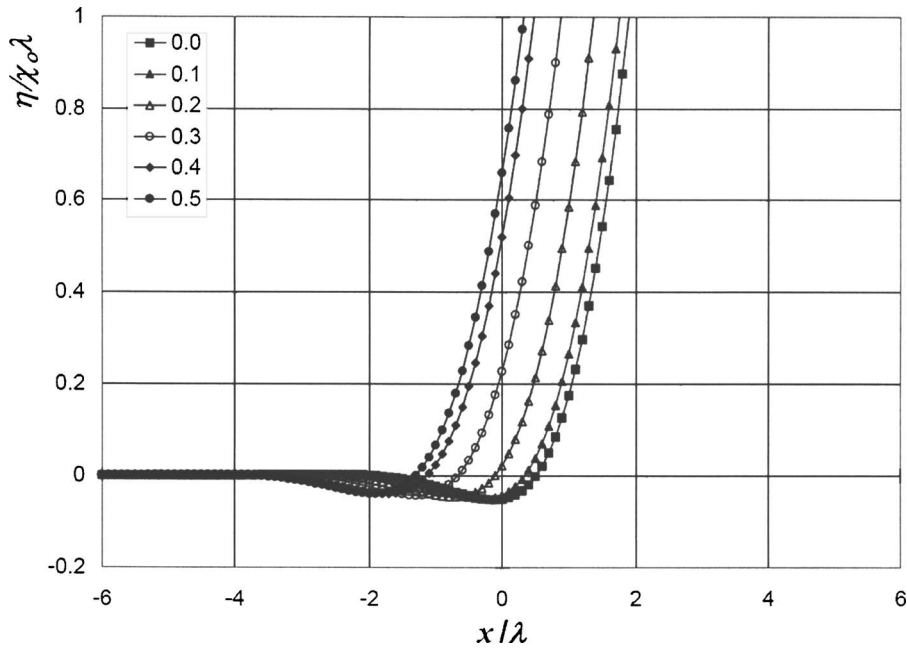
Fig. 2 Normalized elastic curve, $K=10$. Snapshots for $t/T=0,0.1,0.2,0.3,0.4,0.5$; $T=2\pi\omega^{-1}$. $a_0=1$, $\beta_0=0.2$.

$K=10$. Figures 2–5 show local envelopes of normalized elastica, angle, curvature, and shear. Snapshots along a half cycle of harmonic excitation are presented.

Observe from Figs. 3–5 that, at a given section x/λ, angle, curvature, and shear vary cyclically, while the TDP oscillates and the line penetrates into the linear elastic soil, as shown in Fig. 2. The variation observed in the shear force peak is due to dynamic tension oscillation. Figure 6 presents TDP and dynamic tension oscillation during two complete cycles.

Figure 7 shows the corresponding curvature oscillation for several sections, $x/\lambda=-6,-5,\ldots5,6$. Note that, in this particular ex-ample, curvature amplitude attains two maxima, at two distinct sections. The first section, at $x/\lambda\cong-0.7$ (curve with maximum ~0.6), penetrates the soil cyclically, with a curvature variation $\Delta\chi\cong0.6\chi_0$. This is the maximum curvature amplitude. The second section, at $x/\lambda\cong6$, for which $\Delta\chi\cong0.4\chi_0$, does not touch the soil.

Actually, the position where dynamic curvature attains maximum amplitude values depends on the amplitudes and relative phases of TDP excursion and dynamic tension oscillation. An illustrative example is shown in Fig. 8–11. Only the tension ampli-
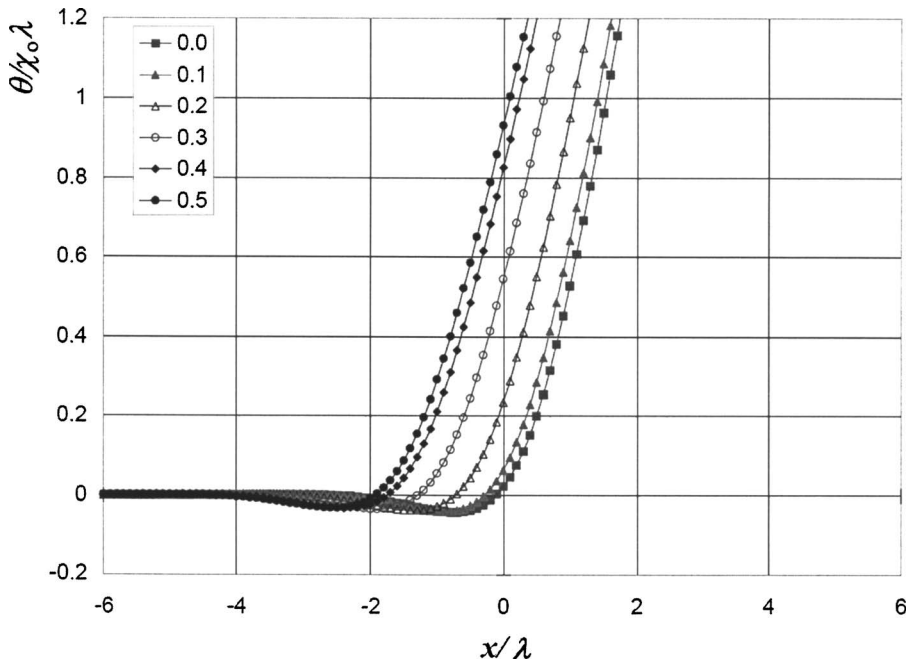

Fig. 3 Normalized angle, $K=10$. Snapshots for $t/T=0,0.1,0.2,0.3,0.4,0.5$; $T=2\pi\omega^{-1}$. $a_0=1$, $\beta_0=0.2$.
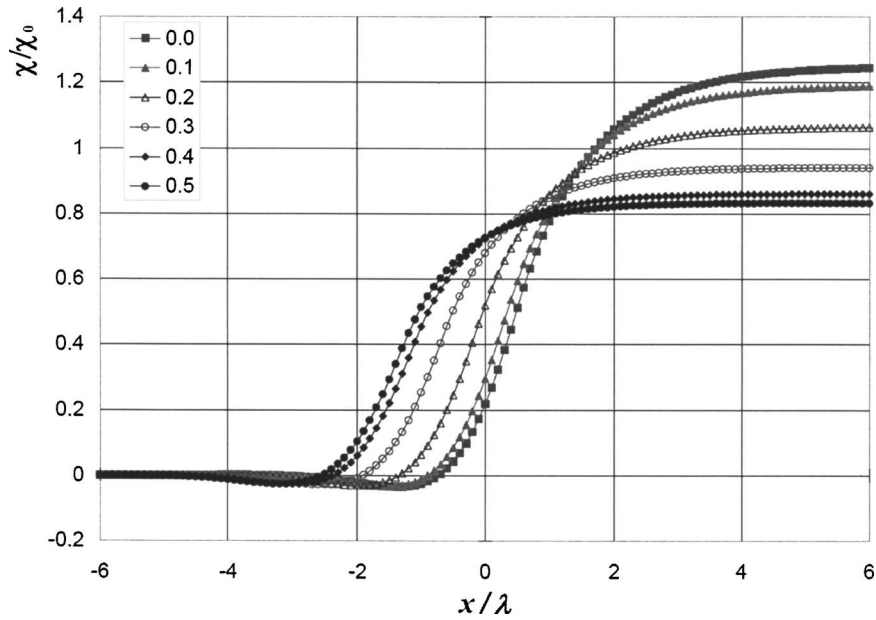
Fig. 4 Normalized curvature, $K=10$. Snapshots for $t/T=0,0.1,0.2,0.3,0.4,0.5$; $T=2\pi\omega^{-1}$. $a_0=1$, $\beta_0=0.2$.

tude was modified, to a somewhat large value, $\beta_0=0.7$. Relative phases were kept the same. This caused the actual TDP position $\xi_K(t)$ to be deviated from a single harmonic, provoking the interlacing aspect shown in Fig. 10, in the elastic curve envelope. Observe also, from Fig. 9 and 11, that the section where curvature attains the maximum amplitude is no longer the same, having moved upward.

The quasi-static solution preserves some nonlinear aspects of the one-sided contact boundary condition. It should be also emphasized that the examples shown represent typical situations when a riser is driven cyclically at the top by the floating unit.

Before numerical comparisons are shown in the next section, Fig. 12–14 address the effect of soil rigidity by taking a very rigid soil, with $K=10,000$. *Note that curvature variation, the most im-portant issue in fatigue analysis, is not too sensitive to soil rigidity, being dominated by global dynamic quantities: the TDP excursion and the dynamic tension.*

The curvature variation attains a maximum $\Delta\chi\cong0.7\chi_0$, at $x/\lambda\cong-0.2$. Obviously, negative curvature is small, as the riser barely penetrates the soil, as shown in Figs. 13 and 14.

Comparison to Full Nonlinear Time-Domain Simulations. The present quasi-static analytical solution has been compared to full nonlinear simulation results, showing a remarkable agreement. In fact, this analytical solution can be viewed as a benchmark for nonlinear simulations, as far as the underlined hypotheses are fulfilled, namely, *subcritical planar dynamics* and *linear elastic soil*. Note that the two dynamic inputs to the analytical
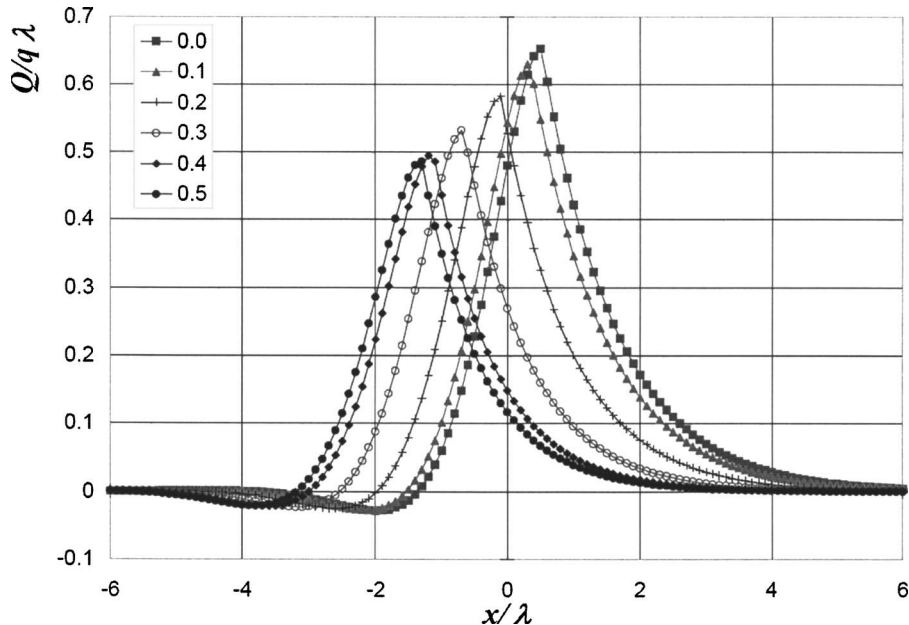

Fig. 5 Normalized shear force, $K=10$. Snapshots for $t/T=0,0.1,0.2,0.3,0.4,0.5$; $T=2\pi\omega^{-1}$. $a_0=1$, $\beta_0=0.2$.
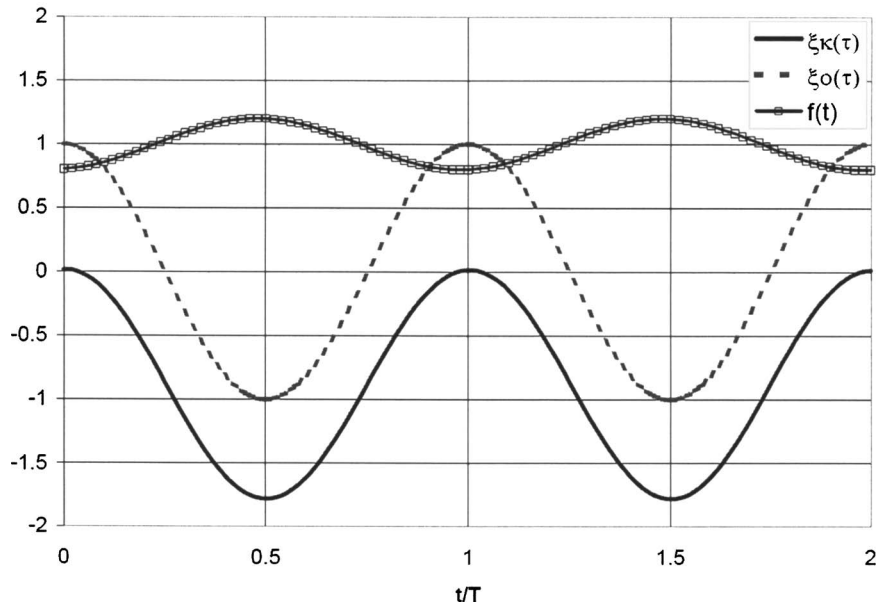
TDP Position and Dynamic Tension

Fig. 6 Normalized TDP excursion and dynamic tension in time: $a_0=1$, $\beta_0=0.2$, $K=10$
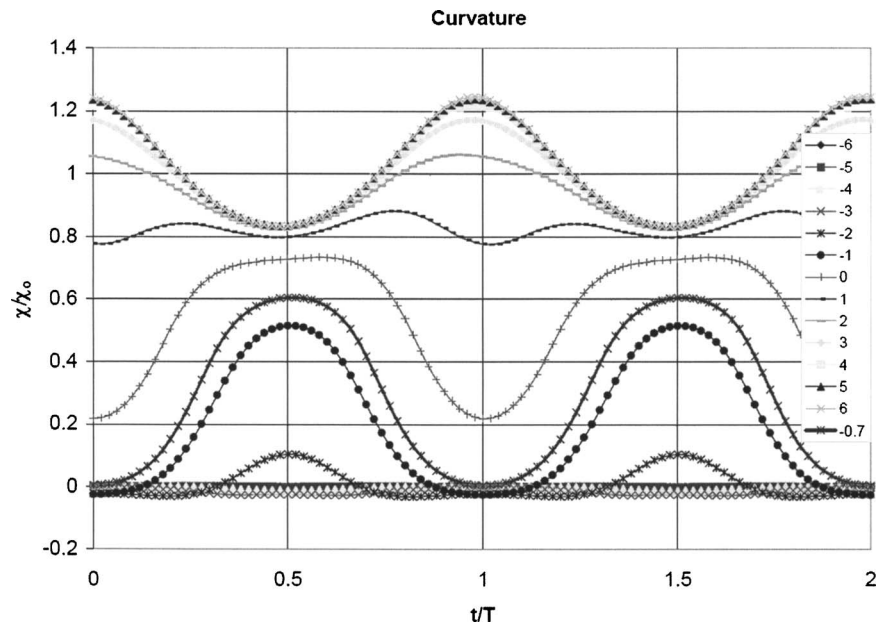
Curvature

Fig. 7 Normalized curvature in time at various sections: $x/\lambda=-6,-5,\ldots,5,6$; $a_0=1$; $\beta_0=0.2$; $K=10$

solution, $x_0(t)$ and $\tau_0(t)$, respectively, the TDP excursion and the dynamic tension at TDP, are not restricted to be sinusoidal. As a matter of fact, they are general and represent the global nonlinear dynamics.

We took a typical 1800 m water depth (a real case) SCR, given in Table 1. The nonlinear simulation code used is specifically dedicated to riser analysis.[4] For simplicity, the nonlinear code was

run in the absence of waves and current, in order to generate typical $x_0(t)$ and $\tau_0(t)$ time series, which are shown in Figs. 15 and 16. Only a clockwise[5] circular motion was imposed to the riser top with an amplitude radius $A=1.5$ m and period $T=10$ s.

Curvature time-histories are compared in Figures 17–19. The

---

[4]ORCAFLEX®, version 8.6.

[5]As shown in Aranha et al. [8], the nonlinear hydrodynamic damping along the riser length causes clockwise and anti-clockwise motions to provoke quite different responses in the dynamic curvature at TDP.
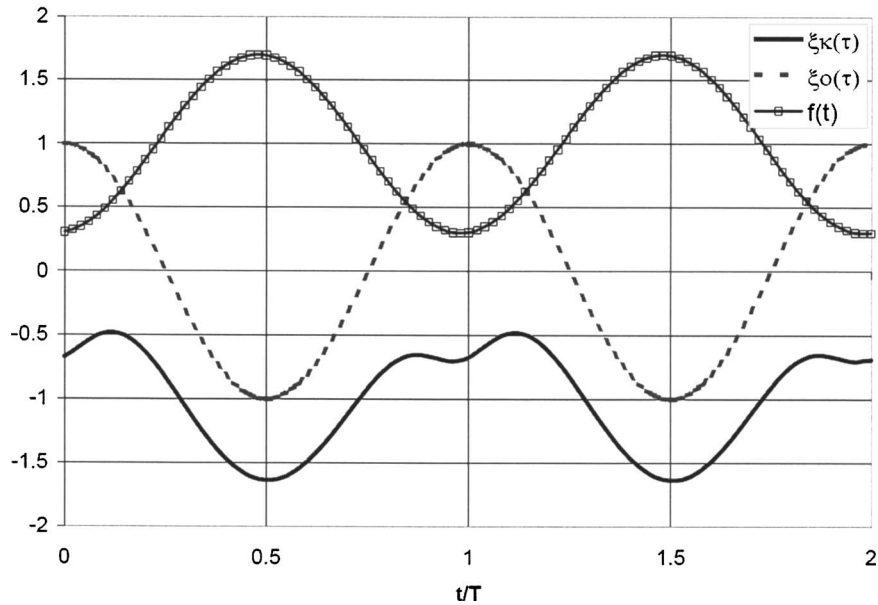
Fig. 8 Normalized TDP excursion and dynamic tension in time: $a_0=1$, $\beta_0=0.7$, $K=10$
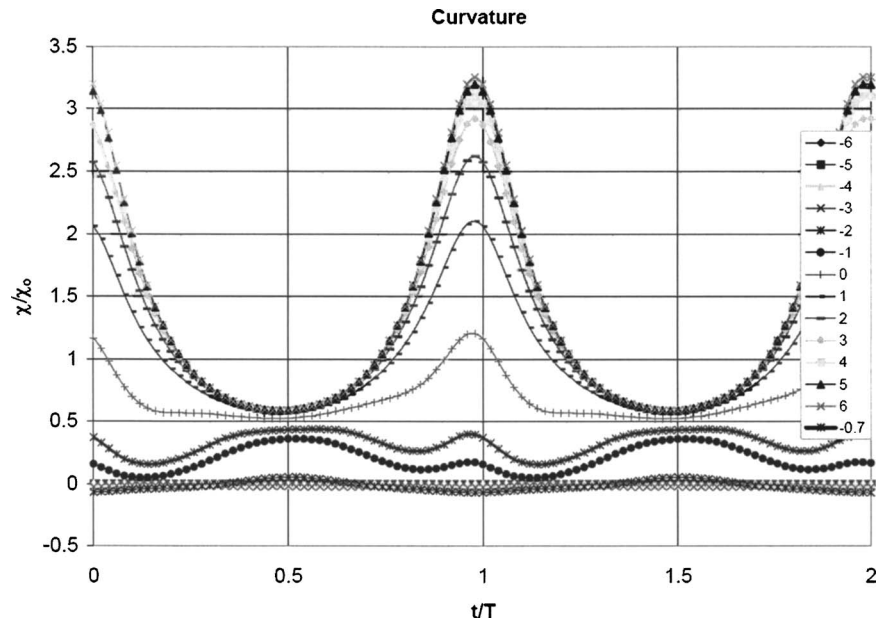

Fig. 9 Normalized curvature in time at various sections: $x/\lambda=-6,-5,\dots,5,6$; $a_0=1$; $\beta_0=0.7$; $K=10$

agreement of the numerical simulation with the analytical solution is indeed remarkable. The nonlinear response caused by the (one-side) contact boundary condition is completely captured by the analytical solution. Figure 17 refers to a section just at what we call a 'critical section,' where the curvature dynamic amplitude attains the maximum value amongst all sections that just touch the soil cyclically. Figures 18 and 19 refer to another typical section ($x/\lambda=-3$), that rests on the soil cyclically. The difference is the soil rigidity, soft in the first case ($K=10$), Fig. 18, and relatively rigid, in the second ($K=1000$), Fig. 19.

Figure 20 shows, for the studied case, the minimum value attained by the dynamic curvature. Figure 20(a) presents the minimum curvature as a function of x/λ, parametrized by the soil rigidity coefficient K. Figure 20(b) shows the minimum value attained along the whole length at TDA, as a function of $\log K$. As can be seen, the minimum curvature is of order of $5\%\chi_0$, for a very soft linear elastic soil, with $K=1$. The sensitivity with respect to soil rigidity is, therefore, very small. It causes insignificant differences in the main curvature variation that is driven by the dynamic tension and the TDP excursion.
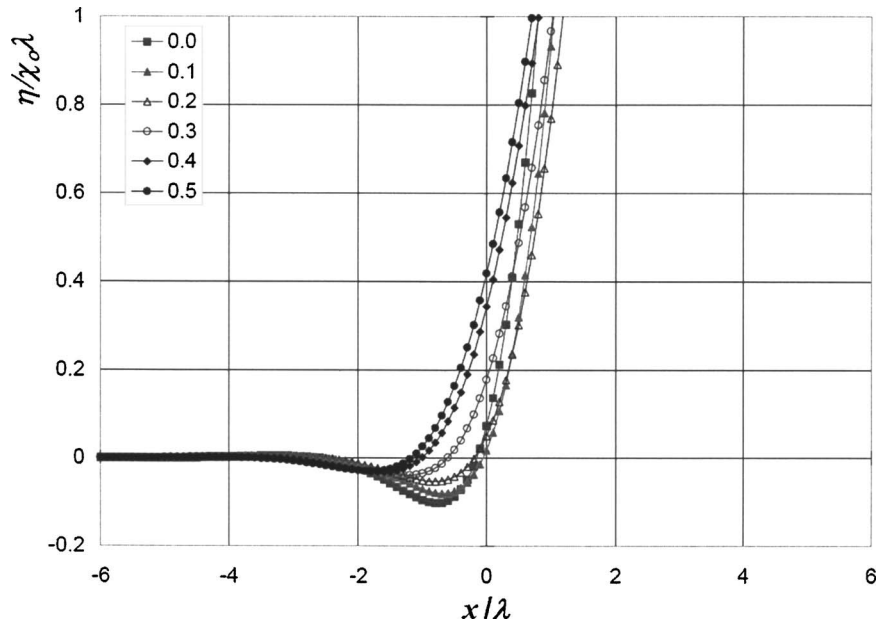
Fig. 10 Normalized elastic curve. $K=10$. Snapshots for $t/T=0,0.1,0.2,0.3,0.4,0.5$; $T=2\pi\omega^{-1}$. $a_0=1$; $\beta_0=0.7$.
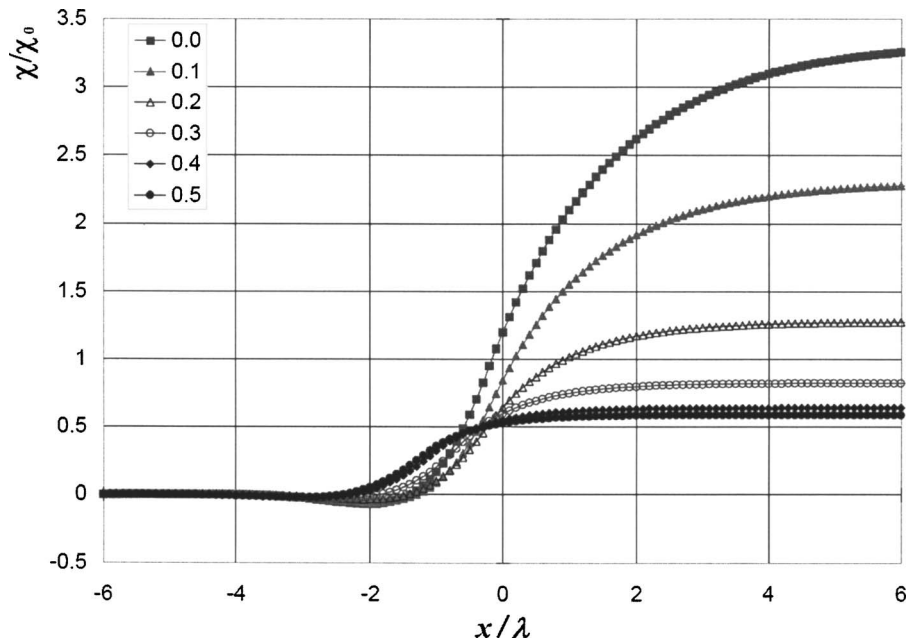

Fig. 11 Normalized curvature. $K=10$. Snapshots for $t/T=0,0.1,0.2,0.3,0.4,0.5$; $T=2\pi\omega^{-1}$. $a_0=1$; $\beta_0=0.7$.

Addressing the Eigenvalue and the VIV Problem (See Fig. 20)

As pointed out before, we could consider a nonlinear eigenvalue problem,[6] taking into account the whole pipe, from the anchor to the floating unit. Or else, an effective participation length on the soil, $L_K(t)$, could be considered and evaluated to be smaller than 10λ. If, instead, only the suspended part is analysed under a

cable dynamics approach, riser flexural rigidity and soil interaction effects must be incorporated. This can be pursued through Eq. (15), given the dynamic tension and the TDP excursion of a corresponding cable. A simple way to evaluate these variables is to use an asymptotic eigenmode solution.

Solution in the Suspend Part. The linear eigenvalue problem of taut inclined cables was thoroughly addressed by Triantafyllou [13], who points out that "…In the case of a taut wire, stretching is of second order, but the elastic stiffness must be finite, other-

---

[6]See, e.g., Burridge et al. [17] for the treatment of a similar problem.
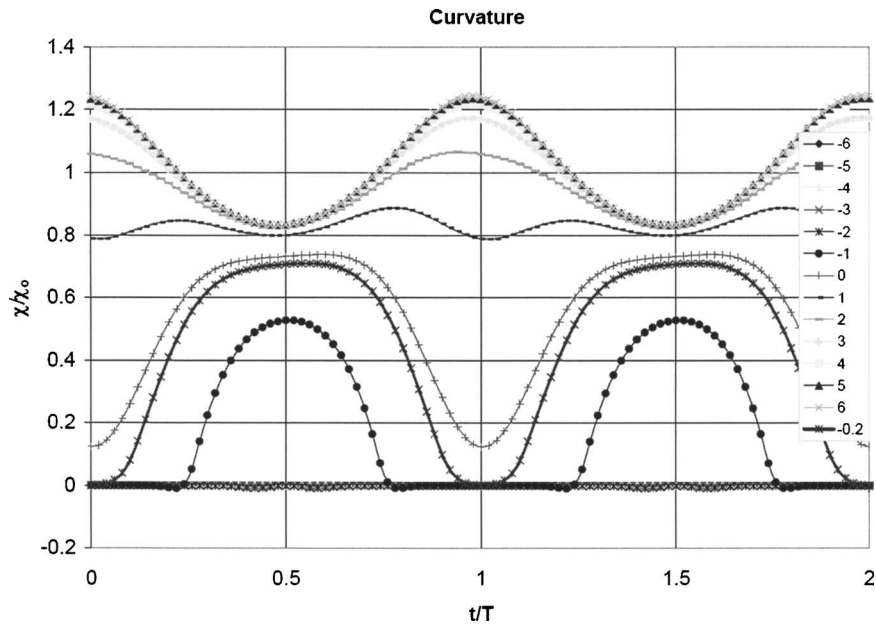
Fig. 12 Normalized curvature in time at various sections: $x/\lambda = -6, -5, \ldots, 5, 6$; $a_0 = 1$; $\beta_0 = 0.2$; $K = 10,000$
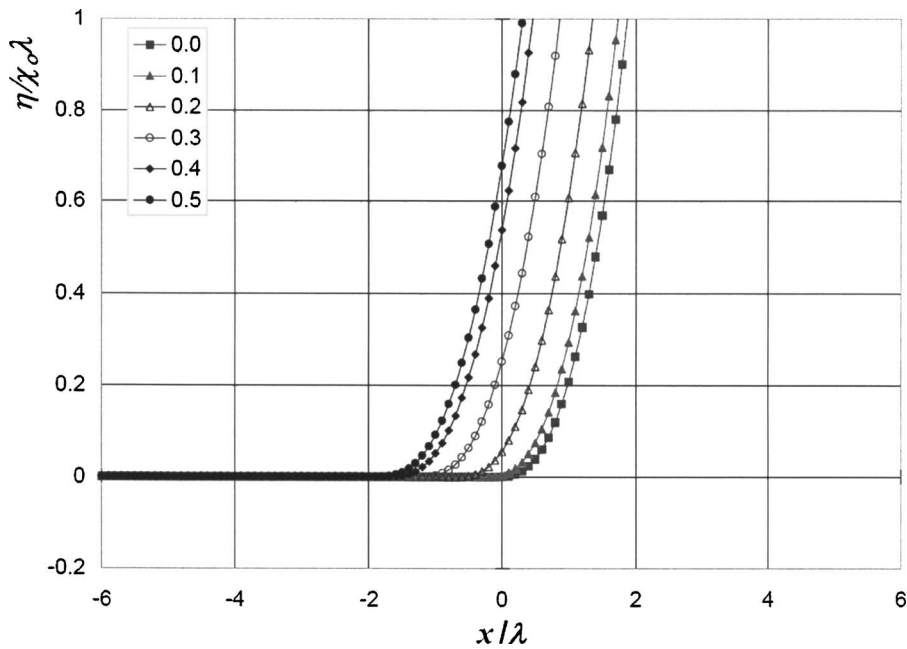

Fig. 13 Normalized elastic curve, $K = 10,000$. Snapshots for $t/T = 0, 0.1, 0.2, 0.3, 0.4, 0.5$; $T = 2\pi\omega^{-1}$. $a_0 = 1$; $\beta_0 = 0.2$.

wise is geometrically impossible to have any vibrations at all. In the case of a sagging cable the elastic stiffness can be infinite, because the cable admits transverse displacements causing second-order tangential displacements by readjusting its curvature and with no stretching." Triantafyllou considers two basic asymptotic solutions. The first one is "weakly varying" in space,[7] compared to the static tension, stretching being mandatory. This solution is given in terms of Airy functions. The dynamic tension is also weakly varying in space and strongly dependent on elastic stiffness (axial rigidity). The second solution is "strongly varying" in space and given as a WKB approximate solution, consistent with assuming an infinite elastic stiffness, i.e., a nonextensible wire. The total solution is a linear combination of both. In the weakly varying solution, elastic stiffness dominates the upper part and curvature the lower part. This fact causes modes to be hybrid, neither symmetric nor anti-symmetric. In fact, a turning point close to the upper end exists in the Airy function solution. Concerning VIV of deep-water steel catenary risers, modes of order

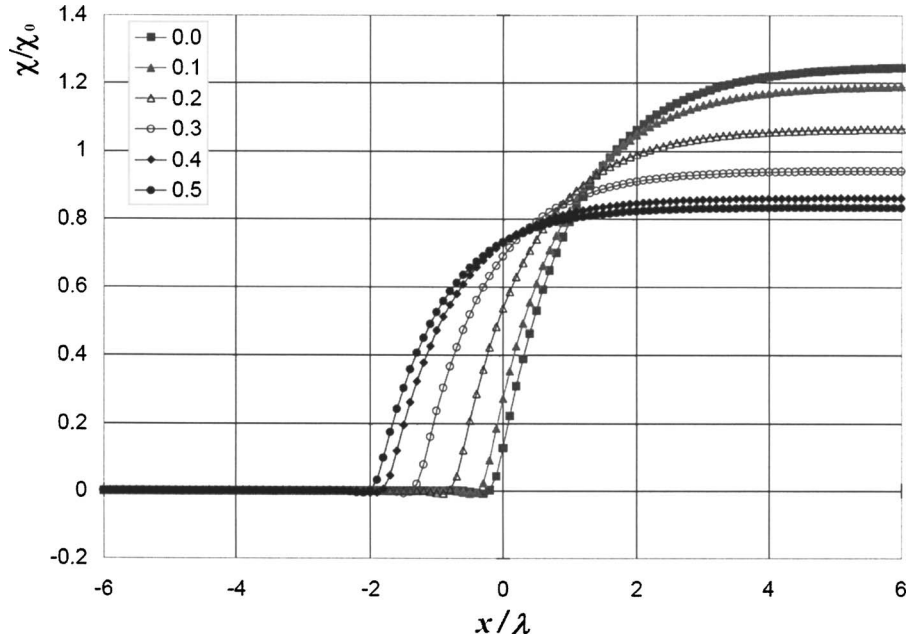[7]Triantafyllou uses the terms "slowly" and "fast" varying in space.

Fig. 14 Normalized curvature, $K=10,000$. Snapshots for $t/T=0,0.1,0.2,0.3,0.4,0.5$; $T=2\pi\omega^{-1}$. $a_0=1$; $\beta_0=0.2$.

20th or higher are likely to occur. Locally, at TDA, kinematics will be dominated by the strongly varying solution in space, the WKB approximation.

WKB Solution (Nonextensible String). Consider a small perturbation around a given static configuration, defined by the functions $T(s)$ and $\theta(s)$. Let $u(s,t)$ and $v(s,t)$ be perturbed *tangential* and *normal* displacements at s. Let also $\tau(s,t)$, $\gamma(s,t)$ be, respectively, small perturbations of effective tension and angle (with respect to horizontal).

Define $\breve{\xi}=s/L=\varepsilon\xi$, $\breve{u}=u/L$, $\breve{v}=v/L$, and $t=tc_0/L=\varepsilon\hat{t}$ as (global) nondimensional quantities. Let then a harmonic solution be given by $\breve{u}(\xi,t)=\psi(\xi)e^{i\omega t}$ and $\breve{v}(\xi,t)=\varphi(\xi)e^{i\omega t}$, where $\omega=\Omega L/c_0=\varepsilon^{-1}\hat{\omega}$. Neglecting viscous and quadratic terms in curvature, as well as the dynamic tension variation, the planar linear eigenvalue problem for the nonextensible string can be written

$$[F(\breve{\xi})\varphi']' + \omega^2\varphi = 0 \qquad (17a)$$

Table 1 Typical SCR data, no current

Axial Rigidity, EA (kN)	2.314×10^6
Bending Stiffness, EI (kN m²)	9915
Immersed weight, q (kN/m)	0.727
m (kg/m) (filled with water)	108.0
External diameter, D (m)	0.2032
Thickness (mm)	19.05
Depth H (m)	1800
Total length (m)	5047
Angle at top, θ_L (deg) (no current)	70 (with respect to horizontal)
Soil Rigidity, k (kN/m/m)	466.37
Suspended length, L (m)	2571
Static tension at TDP, T_0 (kN)	680.55
Flexural length, λ(m)	3.82
Curvature at TDP, χ_0 (m⁻¹)	1.077×10^{-3}
Nondimensional curvature at TDP, $X_0=\chi_0\lambda$	4.114×10^{-3}
Local scale, $\varepsilon=\lambda/L$	1.486×10^{-3}
Nondimensional soil rigidity parameter, $K=kEI/T_0^2$	10

$$\psi(\breve{\xi}) = \omega^{-2}[(1+a)F(\breve{\xi})L\chi(\breve{\xi})]\varphi'(\breve{\xi}) \qquad (17b)$$

where $a=m_a/m$,

$$F(\breve{\xi}) = T(\breve{\xi})/T_0 = [c(\breve{\xi})/c_0]^2 \qquad (18)$$

is the static nondimensional effective tension function and $c(\breve{\xi}) = \sqrt{T(\breve{\xi})/(m+m_a)}$ is the transversal wave celerity of a cable at $\breve{\xi}$.

Equation (17a) is, strictly speaking, the eigenvalue equation. Equation (17b) gives the tangential displacement $\psi(\breve{\xi})$, as a direct linear operation on $\varphi(\breve{\xi})$, a consequence of not considering extensibility. To first order in ω^{-1}, considered a small quantity, WKB technique applied to (17) leads to a general asymptotic form

$$\varphi(\breve{\xi}) \cong F^{-1/4}(\breve{\xi})\left[C_1 \sin\left(\omega\int^{\breve{\xi}} F^{-1/2}(u)du\right) + C_2 \cos\left(\omega\int^{\breve{\xi}} F^{-1/2}(u)du\right) \right] \qquad (19)$$

As pointed out in Pesce et al. [14], these eigenmodes are sinusoidal functions, modulated in phase and amplitude and resemble Bessel's functions. Being $\phi(\breve{\xi})=\omega\int^{\breve{\xi}}F^{-1/2}du$, the phase angle, the nondimensional wave number is given by $\kappa=d\phi/d\breve{\xi}=\omega\sqrt{F(\breve{\xi})}$. In other words, $c(\breve{\xi})/c_0=\omega/\kappa$, a classical result in dispersive waves theory (see, e.g., [18], p. 365). If $F(\zeta)=F_0$, a constant, there would be no dispersion at all.

Applying, e.g., a pinned-pinned boundary condition, such that $\varphi(0)=\varphi(1)=0$, we get

$$\varphi_n(\breve{\xi}) \cong A_n F^{-1/4}(\breve{\xi})\sin\left(\omega_n\int_0^{\breve{\xi}} F^{-1/2}(u)du\right)$$

$$\psi_n(\breve{\xi}) \cong \omega^{-1}(1+a)A_n L\chi(\breve{\xi})F^{1/4}(\breve{\xi})\cos\left(\omega_n\int_0^{\breve{\xi}} F^{-1/2}(u)du\right)$$
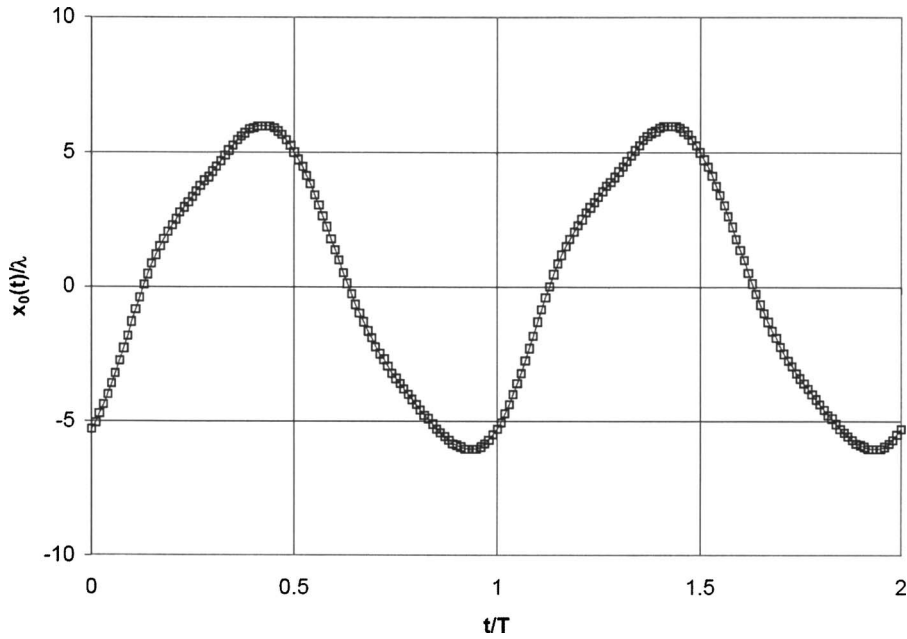
Fig. 15 Nonlinear numerical simulation. Normalized TDP excursion, $x_0(t)/\lambda$, of a typical SCR.
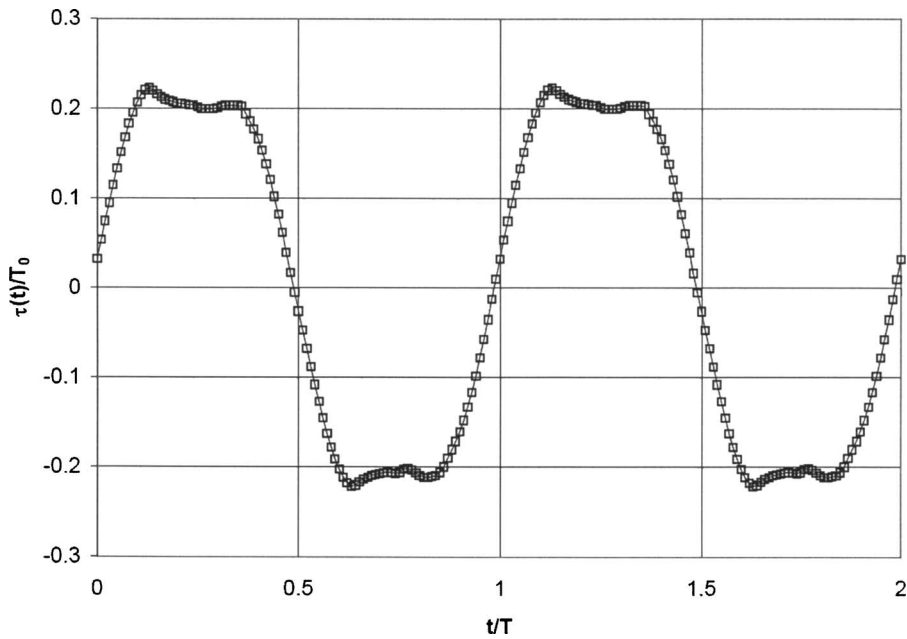

Fig. 16 Nonlinear numerical simulation. Normalized dynamic tension, $\tau_0(t)/T_0$, at TDP of a typical SCR.

$$\omega_n \cong n\pi \left(\int_0^1 \frac{d\breve{\xi}}{\sqrt{F(\breve{\xi})}} \right)^{-1} \tag{20}$$

In this case, the (dimensional) natural frequencies are given by

$$\Omega_n = \omega_n \frac{c_0}{L} = \omega_n \frac{1}{L} \sqrt{\frac{T_0}{(m+m_a)}} \tag{21}$$

Figures 21 and 22 present the WKB approximate solution corresponding to a typical SCR compared to a finite element method solution. General data is found in Table 1. Figure 21 shows the 25th eigenmode and Fig. 22 presents the corresponding natural frequencies, numerically assessing the extensibility[8] effect. As expected, for relatively high-order modes, the WKB solution (strongly varying in space) approximates the solution quite well in TDA region.

Note from (20) that at the lower pinned end, dynamic curvature is really small, of second-order, as should be expected. The WKB approximation predicts that the largest dynamic curvature occurs
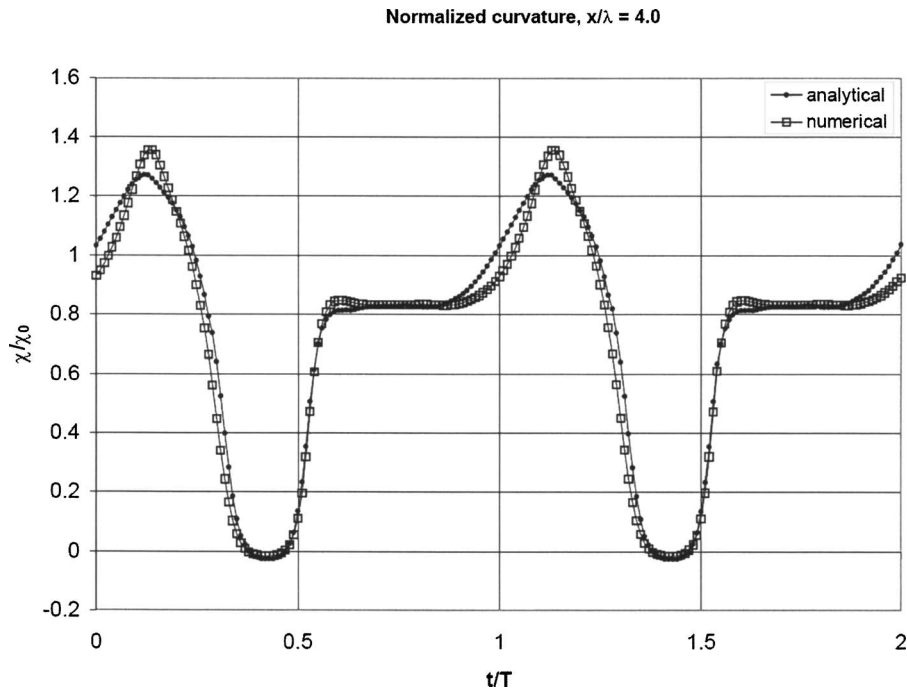
---

[8]See, also, [19].

Fig. 17 Curvature time histories at $x/\lambda = 4.0$, at the critical section. Analytical and numerical solutions, $K=10$.
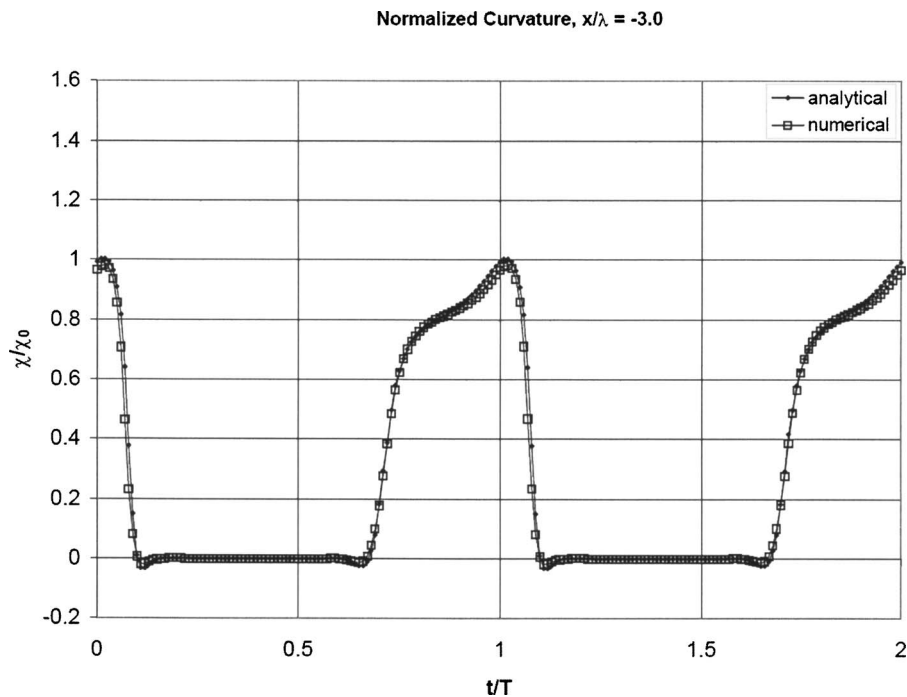

Fig. 18 Curvature time histories at $x/\lambda = -3$, a section that rests on the soil cyclically. Analytical and numerical solutions, $K=10$.

at a suspended section of the riser where the eigenmode first peaks. The open point is to evaluate the dynamic curvature at TDA, by locally correcting the WKB solution under the effects of bending stiffness and soil rigidity.

Local Flexural Rigidity Effect at TDA on a Linear Elastic Soil: A Quasi-Static Approach. We follow the reasoning presented before by considering the dynamics of the supported part

on the soil dominated by the dynamics of the suspended part. In other words, the dynamic response of the supported part is considered quasi static. For this we must restrict ourselves to the case where $K \gg \omega$; $K = kEI/T_0^2$ and $\omega = \Omega L/c_0 = \varepsilon^{-1}\hat{\omega}$.

Under this hypothesis, consider the riser vibrating in a particular high-order mode. No motion is imposed at the upper extremity. Apart the transition region in the TDA, the suspended part dynam-
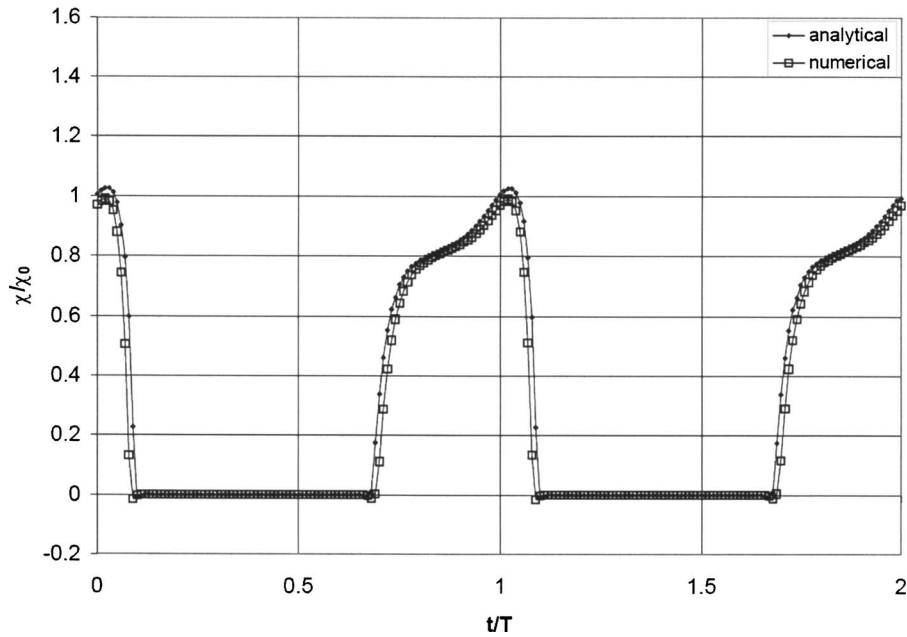
Fig. 19 Curvature time histories at $x/\lambda=-3$. Analytical and numerical solutions, $K=1000$.

ics is considered globally, described by the asymptotic approximation, with a hinge placed at the static TDP of the corresponding string, as given by Eq. (20). If a real tangency condition is considered, the excursion of the TDP might be evaluated from the pinned case, to first order in $X_0=\chi_0\lambda$, as $x_0(t) \cong \gamma(0,t)/\chi_0$. In nondimensional form, at space and time scales (ξ,t), we could then write, $\xi_0(t) \cong \gamma(\xi,t)/(\chi_0\lambda)$. Locally, the dynamics of the suspend part is represented through $x_0(t)$ and $\tau(0,t)$ or, in nondimensional form, through $\xi_0(t)$ and $f(t)$. Therefore, if $K \gg \max[f(t)]$ and an impact against the soil is precluded, such that $M=|\dot{x}_0/c_0| < 1$, i.e.,

$$\varepsilon |d\xi_0/dt| < 1 \qquad (22)$$

then the quasi-static approximation (Eqs. (15) and (16)) apply, given $\xi_0(t)$ and $f(t)$. To evaluate $\xi_0(t)$ and $f(t)$, recall the classical dynamic equations for a suspended string

$$\frac{\partial \tau}{\partial s} - \gamma T(s)\chi(s) = m\frac{\partial^2 u}{\partial t^2}$$

$$\tau\frac{d\theta}{ds} + \frac{\partial}{\partial s}(\gamma T) = (m + m_a)\frac{\partial^2 v}{\partial t^2}$$

$$\frac{\partial u}{\partial s} - v\chi(s) = e$$

$$\frac{\partial v}{\partial s} + u\chi(s) = \gamma \qquad (23)$$

where $e=e(s,t)$ is the dynamic axial deformation. Let $u=u/\lambda =\varepsilon^{-1}\breve{u}$ and $v=v/\lambda=\varepsilon^{-1}\breve{v}$ be the nondimensional displacements in local coordinates. If the string is considered nonextensible, such
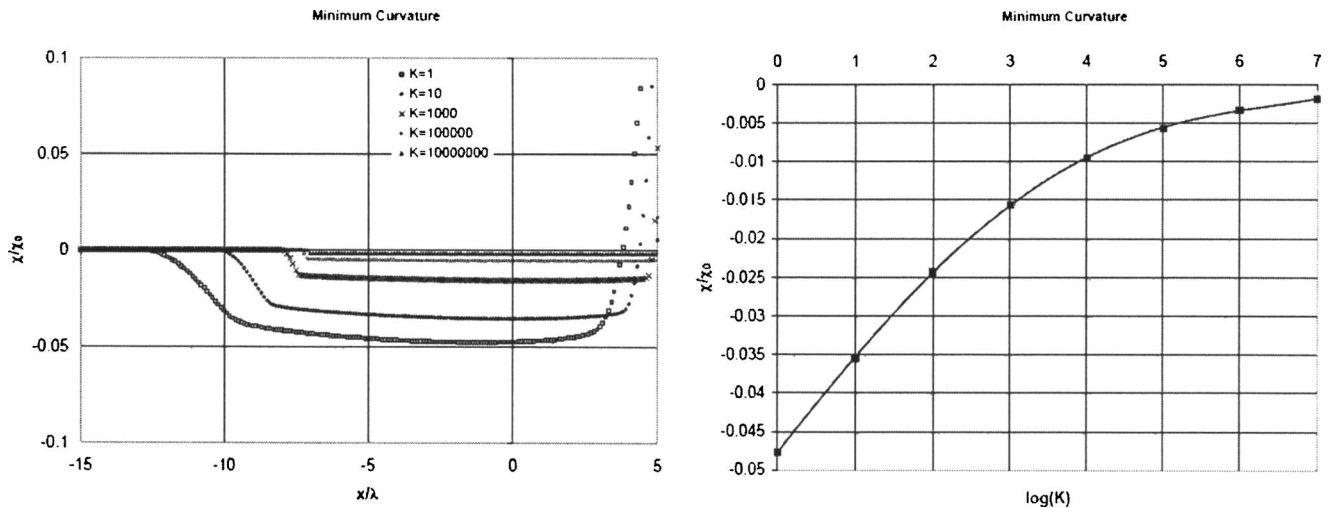

Fig. 20 Normalized curvature. Minimum value: (*a*) along the length and (*b*) as a function of the soil rigidity parameter *K*.
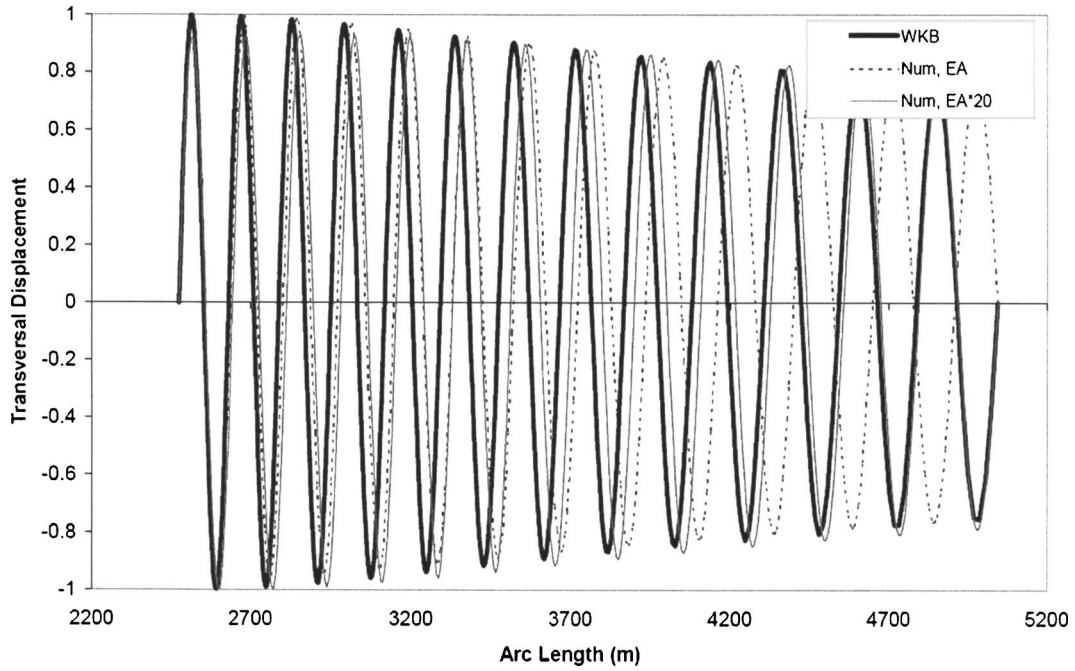
Transversal Displacement - Mode 25

Fig. 21 WKB approximate solution compared to numerical results obtained by a standard finite element method. Free-hanging SCR. No current. θ_L=70 deg. Assessing the extensibility effect.

Natural Frequencies for a Catenary Riser; WKB compared to numerical approach
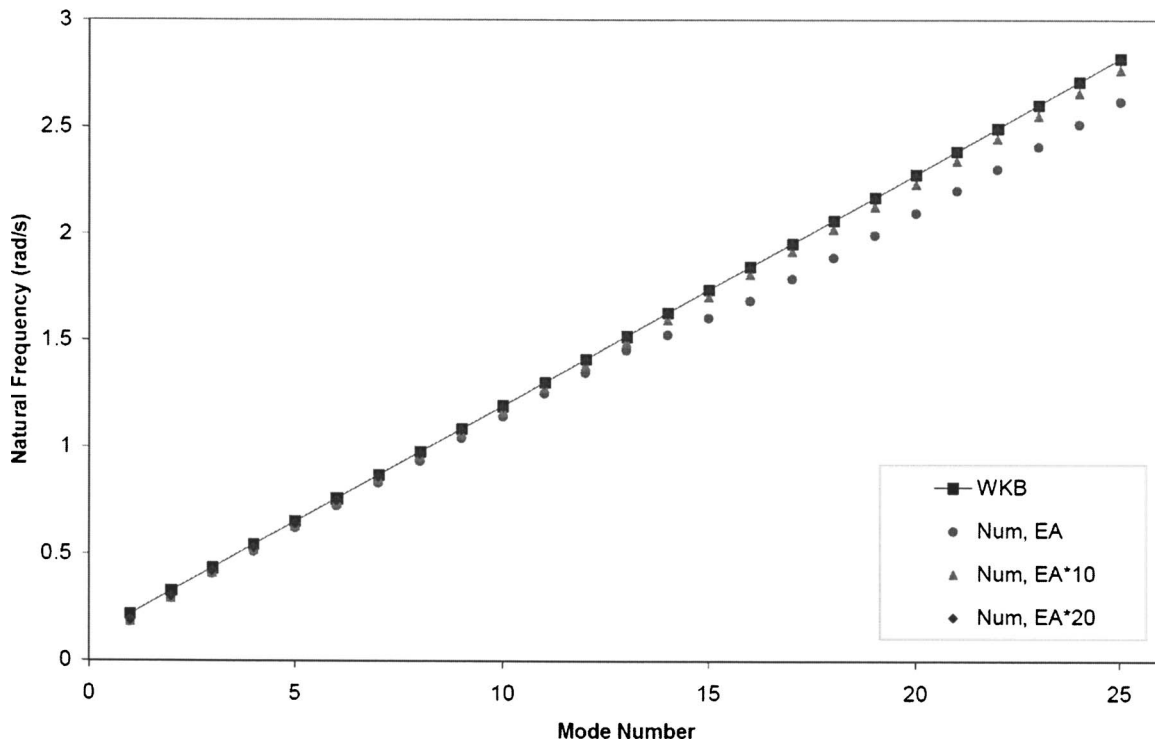

Fig. 22 Natural frequencies of a SCR. Assessing the extensibility effect. Numerical solution, with three different values of axial rigidity, compared to the WKB analytical approximation. No current; θ_L=70 deg.
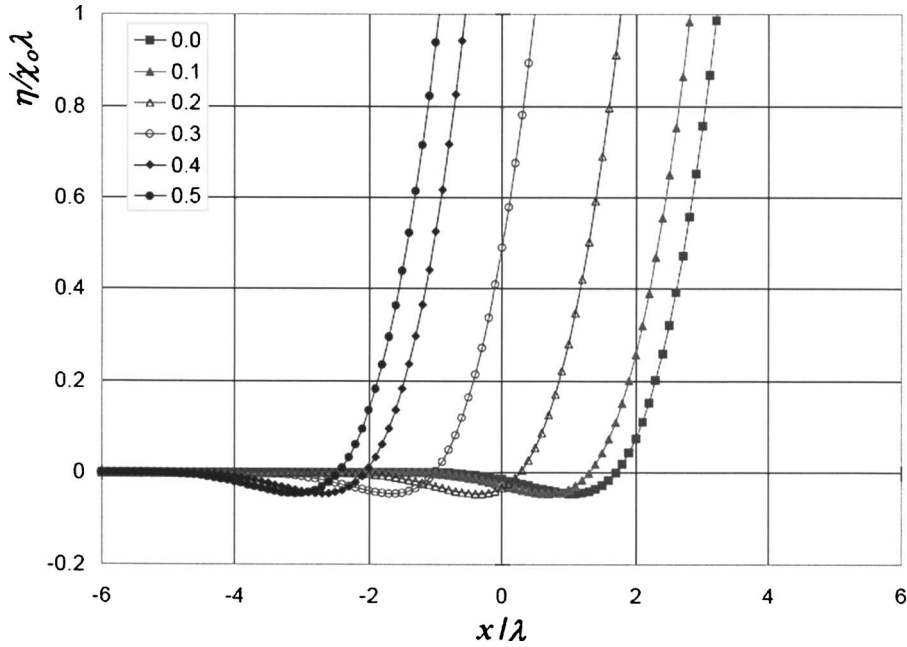
Fig. 23 Normalized elastic curve, $K=10$. Snapshots for $t/T=0,0.1,0.2,0.3,0.4,0.5$; $T=2\pi\omega^{-1}$. $a_0=2.08$; $\beta_0\approx O(10^{-6})$.

that $e(s,t)\equiv 0$, then the following nondimensional equations are obtained for $\gamma(\xi,t)$, $\xi_0(t)$, and $f(t)$:

$$\gamma(\xi,t) = \frac{\partial v}{\partial \xi} + \frac{1}{1+a}\int_0^\xi X(\xi)v(\xi)d\xi \tag{24}$$

$$\xi_0(t) \cong \frac{1}{X_0}[\gamma(X,t)]_{\xi\to 0^+} \tag{25}$$

$$f(t) \cong 1 - \frac{1}{X_0}\left[\frac{\partial(\gamma F)}{\partial \xi} - \varepsilon^2\frac{\partial^2 v}{\partial t^2}\right]_{\xi\to 0^+} \tag{26}$$

Note that, if extensibility had been taken into account, the dynamic tension would follow the weakly varying Airy solution, being strongly dependent on the elastic stiffness, such that $\tau(s,t)\cong EAe$. Therefore, Eq. (26) gives a poor estimate for the dynamic tension. Nevertheless, as kinematics at TDA is dominated by the WKB solution, Eq. (25) is a good estimate for the TDP excursion. Let the transversal displacement be given by $v = \alpha\varphi(\xi,t)\cos\omega t$, where $\alpha=A/\lambda$ is the nondimensional modal amplitude. Observe that

$$\varphi^I(\xi) = \frac{d\varphi}{d\xi} = \varepsilon\frac{d\varphi}{d\check{\xi}}$$

$$\varphi^{II}(\xi) = \frac{d^2\varphi}{d\xi^2} = \varepsilon^2\frac{d^2\varphi}{d\check{\xi}^2} \tag{27}$$

and that, for a catenary riser, $F(\theta(\xi))\cong\sec\theta(\xi)$. Now, using the WKB approximation given by (20), such that, to first order in ω^{-1},

$$\frac{d\varphi}{d\check{\xi}} \cong \omega[F(\check{\xi})]^{-3/4}\cos\left\{\omega\int^{\check{\xi}}[F(\check{\xi})^{-1/2}]d\check{\xi}\right\}$$

$$\frac{d^2\varphi}{d\check{\xi}^2} \cong -\omega^2\varphi(\check{\xi}) \tag{28}$$

a first-order approximation is obtained for $\xi_0(t)$ and $f(t)$, as

$$\xi_0(t) \cong \varepsilon\omega X_0^{-1}\alpha\cos\omega t \tag{29}$$

and

$$f(t) \cong 1 - \varepsilon\omega X_0\alpha\cos\omega t \tag{30}$$

Observe that the dynamic amplitude of $\xi_0(t)$ is X_0^{-2} larger than the dynamic amplitude of $f(t)$. This is a direct consequence of not considering extensibility.[9] Note also that the non-impact condition (22) restricts the present analysis to

$$M = \varepsilon^2\omega^2 X_0^{-1}\alpha < 1 \tag{31}$$

Equations (29) and (30) may now be applied to the local quasi-static solution, given by Eqs. (15) and (16).

Consider the typical deep water SCR, shown in Table 1. An out-of-plane current is considered and an approximate dynamic solution is taken, such that VIV occurs in the catenary plane.[10] We take the modal amplitude as $A=1.0D$, a common peak value encountered in VIV analysis of flexible cylinders in water (see, e.g., [20]). In the present case, $\alpha=A/\lambda=0.053$ and $M=0.288\times 10^{-6}\omega^2$. Then, from Fig. 16, we obtain, $\Omega_{25}\cong 2.9$ rad/s and $\omega_{25}=(L/c_0)\times\Omega_{25}=37.038\times\Omega_{25}\cong 107.4$. It can be easily verified that mode 25th locks-on (actually peaks) at a current speed[11] $U=0.5$ m/s. The nonimpact condition is not violated, since $M=0.33$ in this case. Moreover, under the WKB approximation, Eq. (20) shows, explicitly, that eigenfrequencies increase linearly with mode number. Actually, Fig. 21 shows that if the extensibility were considered, the increasing rate would depart from the linear rate. From Eq. (31), the nonimpact condition is violated if $\omega^2 \geqslant \varepsilon^{-2}X_0\alpha^{-1}$. In the present case, this would happen from mode 44th on. Figures 23–25 present for mode 25th snapshots ($t/T=0,0.1,0.2,0.3,0.4,0.5$; $T=2\pi\omega^{-1}$) of the local elastica, curvature, and shear. Figure 26 shows curvature with time.

Curvature variation attains a maximum, $\Delta\chi\cong\chi_0$, at $\xi=x/\lambda\cong 0.4$, as shown in Figs. 24 and 25. Moreover, from Eqs. (27),

---

[9]Though relatively poor, this estimate is generally in the safe side, as dynamic tension usually reduces dynamic curvature.

[10]Actually, the transverse current makes the elastica to depart from the vertical plane.

[11]In fact, the reduced velocity takes the value $^{25}V_r=2\pi U/\Omega_{25}D\cong 5.3$.
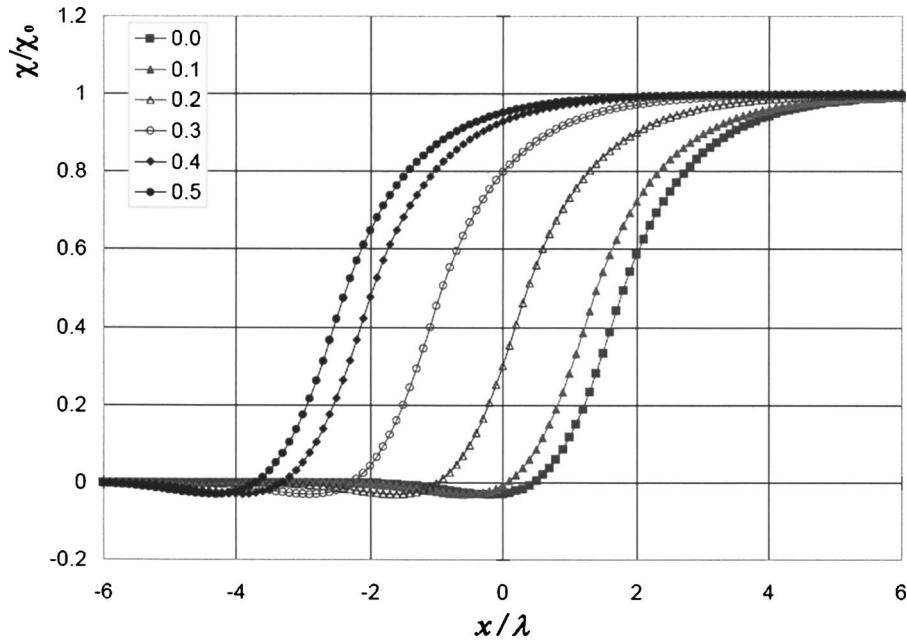
Fig. 24 Snapshots of the normalized curvature, $K=10$. $a_0=2.08$; $\beta_0 \approx O(10^{-6})$.

(28), and (20) it can be easily shown that the nondimensional amplitude of dynamic curvature at the section $[\xi^*=\varepsilon^{-1}\check{\xi}^* \approx \pi/(2\varepsilon\omega)]$, where the WKB eigenmode approximation has a first anti-node, is of order $X_{\mathrm{WKB}_{\mathrm{max}}} \approx O(MX_0)$. In the present case, the corresponding curvature variation is $\Delta\chi_{\mathrm{WKB}_{\mathrm{max}}} \approx O(2M\chi_0)$ $=0.66\chi_0$, at $\xi^* \approx 10$, a value lower than that evaluated at TDA. Observe also that, as WKB solution underestimates the dynamic tension, the values of shear force peaks do not vary along the cycle.

Conclusions

This paper addressed the riser-soil interaction problem and extended previous results, obtaining a quasi-static analytical solution for the local dynamics of a catenary riser at touchdown region. The present solution is quasi static in the sense that the local

dynamics is governed by the relatively slow dynamics of the suspended part. This is valid if soil rigidity is sufficiently large and if the motion is not so fast as to provoke impact of the riser against the soil. Even though the soil was modeled as linear elastic, the main features of the nonlinear nature of the contact was preserved, by properly considering the oscillatory excursion of the TDP and the dynamic tension.

The local response is given in time domain and depends only on one static parameter, the static tension at TDP, and on two global dynamic functions: the tension and the TDP excursion. The analytical solution was then compared to numerical results obtained from full nonlinear time-domain simulations for a real SCR case. The agreement is remarkably good, showing not only the benchmark value of the present analytical solution. As far as linear soil stiffness and planar dynamics hypotheses may be considered valid, it also shows that penetration in the soil is small and
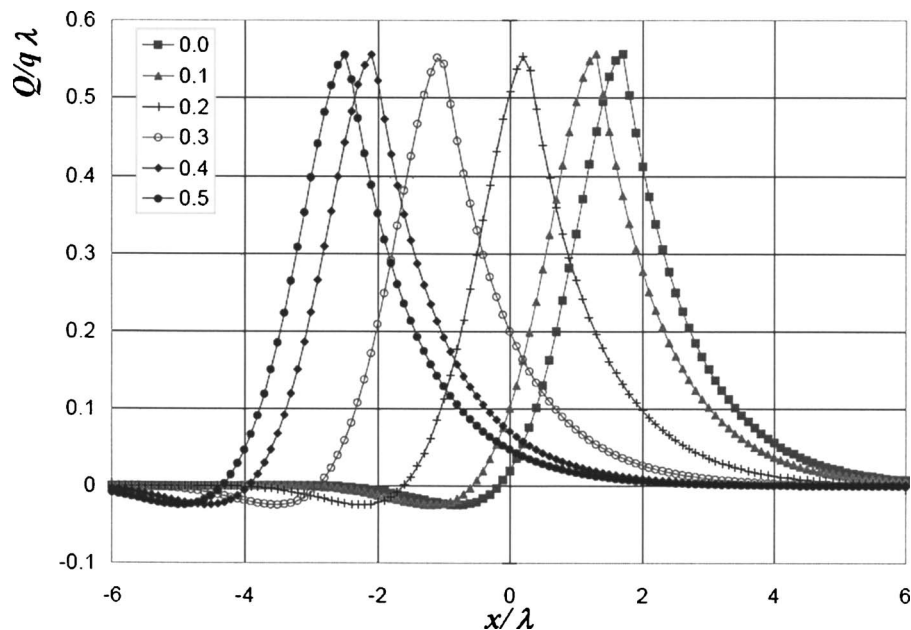

Fig. 25 Snapshots of the normalized shear force, $K=10$. $a_0=2.08$; $\beta_0 \approx O(10^{-6})$.
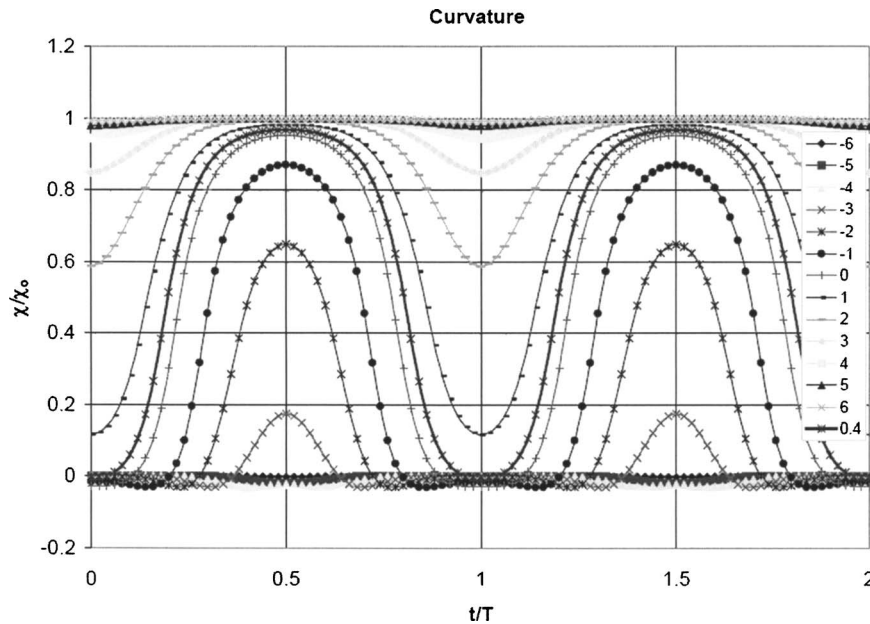
Fig. 26 Normalized curvature in time at various sections, $x/\lambda = -6, -5, \ldots, 5, 6$; $a_0 = 2.08$; $\beta_0 \approx O(10^{-6})$; $K = 10$

that its effect does not change significantly the bending loading that is mainly caused by the cyclic excursion of the TDP and corresponding dynamic tension.

The quasi-static analytical approximation was then merged with an eigenvalue WKB approximate solution, asymptotically valid for a nonextensible suspended cable, providing an analytical tool to deal with the evaluation of the local dynamics, as that possibly caused by vortex-induced vibration in a particular locked-on mode. The WKB approximation gives good estimates for TDP excursion. As the dynamic tension caused solely by VIV is very small, the merged approximate solution may be used as a first estimate of the curvature variation at TDP in the cases of current perpendicular to the riser plane.

The present result can be improved by considering extensibility effects on the dynamic tension. The weakly varying solution in space, given in terms of Airy functions [13], should be considered.[12] Additionally, many other issues remain to be explored further as nonlinear riser-soil interaction phenomena, including embedding, suction, and shocking—all of them outside the present underlined hypotheses.

Acknowledgment

References

[1] Patel, M. H., and Seyed, F. B., 1995, "Review of Flexible Riser Modelling and Analysis Techniques," Eng. Struct., **17**(4), pp. 293–304.

[2] Pesce, C. P., and Martins, C. A., 2005, "Numerical Computation of Riser Dynamics," *Numerical Modelling in Fluid-Structure Interaction*, Advances in Fluid Mechanics Series, S. Chakrabarti ed., WIT Press, Southampton, UK, Chap. 7, pp. 253–309.

[3] Giertsen, E., Verley, R., and Schroder, K., 2004, "CARISIMA a Catenary Riser/Soil Interaction Model for Global Riser Analysis," ASME 23rd International Conference on Offshore Mechanics and Arctic Engineering, Vancouver, Canada, June 20–25, ASME Paper No. OMAE2004-51345.

[4] Leira, B. J., Passano, E., Karunakaran, D., and Farnes, K-H., 2004, "Analysis Guidelines and Application of a Riser-Soil Interaction Model Including Trench Effects," ASME 23rd Int. Conference on Offshore Mechanics and Arctic Engineering, June 20–25, Vancouver, ASME Paper No. OMAE2004-51527.

[5] Fontaine, E., Nauroy, J. F., Foray, P., Roux, A., and Gueveneux, H., 2004, "Pipe-Soil Interaction in Soft Kaolinite: Vertical Stiffness and Damping," 14th International Offshore and Polar Engineering Conference, Vol. 2, pp. 517–524.

[6] Triantafyllou, M. S., Bliek, A., and Shin, H., 1985, "Dynamic Analysis as a Tool for Open Sea Mooring System Design," Annual Meeting of The Society of Naval Architects and Marine Eng., New York.

[7] Irvine, M., 1992, "Local Bending Stress in Cables," *Proc. of 2nd Int. Offshore and Polar Engineering Conference*, San Francisco, June 11–19, ISOPE, Golden, CO, Vol. 2, pp. 342–345.

[8] Aranha, J. A. P., Martins, C. A., and Pesce, C. P., 1997, "Analytical Approximation for the Dynamic Bending Moment at the Touchdown Point of a Catenary Riser," Int. J. Offshore Polar Eng., **7**(4), pp. 293–300.

[9] Pesce, C. P., Aranha, J. A. P., Martins, C. A., Ricardo, O. G. S., and Silva, S., 1998, "Dynamic Curvature in Catenary Risers at the Touchdown Point: An Experimental Study and the Analytical Boundary Layer Solution," Int. J. Offshore Eng., **8**(4), pp. 302–310.

[10] Pesce, C. P., Aranha, J. A. P., and Martins, C. A., 1998, "The Soil Rigidity Effect in the Touchdown Boundary Layer of a Catenary Riser: Static Problem," 8th Int. Offshore and Polar Engineering Conference, Montreal, May 24–29, 1998, Vol. II, pp. 207–213.

[11] Kevorkian, J., and Cole, J. D., 1981, *Perturbation Methods in Applied Mathematics*, Applied Mathematical Sciences Vol. 34, Springer-Verlag, New York.

[12] Bender, C. M., and Orszag, S. A., 1978, *Advanced Mathematical Methods for Scientists and Engineers*, International Series in Pure and Applied Mathematics, McGraw-Hill, New York.

[13] Triantafyllou, M. S., 1984, "The Dynamics of Taut Inclined Cables," Q. J. Mech. Appl. Math., **37**(3), pp. 431–440.

[14] Pesce, C. P., Fujarra, A. L. C., Simos, A. N., and Tannuri, E. A., 1999, "Analytical and Closed Form Solutions For Deep Water Riser-Like Eigenvalue Problem," 9th Int. Offshore and Polar Engineering Conference, Brest, France, June 1–6, Vol. II, pp. 255–263.

[15] Aranha, J. A. P., Pinto, M. O., and Silva, R. M. C., 2001, "On the Dynamic Compression of Risers: An Analytic Expression for the Critical Load," Appl. Ocean. Res., **23**(2), pp. 83–91.

[16] Ramos Jr., R., and Pesce, C. P., 2003, "A Stability Analysis of Risers Subjected to Dynamic Compression Coupled With Twisting," ASME J. Offshore Mech. Arct. Eng., **125**, pp. 183–189.

[17] Burridge, R., Kappraff, J., and Morshedi, C., 1982, "The Sitar String: A Vibrating-String With a One-sided Inelastic Constraint," SIAM J. Appl. Math., **42**(6), pp. 1231–1251.

[18] Whitham, G. B., 1974, *Linear and Non-linear Waves*, Pure and Applied Mathematics, Wiley, New York.

[19] Chucheepsakul, S., and Huang, T., 1997, "Effect of Axial Deformation on Natural Frequencies of Marine Risers," 7th Int. Offshore and Polar Engineering Conference, Honolulu, May 25–30, Vol. II, pp. 131–136.

[20] Williamson, C. H. K., and Govardhan, R., 2004, "Vortex-Induced Vibrations," Annu. Rev. Fluid Mech., **36**, pp. 313–455.

[21] Aranha, J. A. P., and Pinto, M. M. O., 2001, "Dynamic Tension in Risers and Mooring Lines: An Algebraic Approximation for Harmonic Excitation," Appl. Ocean. Res., **23**(2), pp. 83–91.

---

[12]See also [21] for a similar problem on dynamic tension.